A Hybrid BBO and Gradient Descent Method to Reduce Phase Imbalances and Transformer Overloads

Moussa Ahmat[1, 3], Memtine Ndong Augustin[1], Amir Moungache[2], Kidmo Kaoga Dieudonné[1, a)]

[1]*National Advanced School of Engineering of Maroua, University of Maroua, P.O. Box 46 Maroua, Cameroon.*
[2]*Laboratory of Information and Communication Technologies, Faculty of Exact and Applied Sciences of Farcha, University of N'djamena, N'djamena, Chad.*
[3]*Higher Teachers' Training College of Bongor, University of Bongor, Chad.*

[a)] *Corresponding author: kidmokaoga@gmail.com*

Abstract. Distribution networks suffer transformer overloads and phase imbalance, exacerbated by sparse load measurements. We propose a data-robust hybrid optimization framework that couples Biogeography-Based Optimization (BBO) for global exploration with gradient descent for local refinement to allocate transformer loading and balance phases under uncertainty. In simulation studies, the method reduces phase imbalance by 49.99%, cuts overloaded transformers by 28.71% (from 68%), and lowers underloaded units by 10.86% (from 18%). The framework accommodates incomplete daily profiles, enhances reliability, mitigates energy losses and equipment degradation, and supports scalable deployment for grid operations. By uniting metaheuristic robustness with analytical rigor, it offers a practical pathway to extend asset lifespan, reduce maintenance costs, and improve service quality. This work establishes a foundation for data-efficient optimization in distribution systems and paves the way for adaptive, self-healing grids.

INTRODUCTION

The optimal operation of modern electrical distribution networks hinges on effective load management and phase balancing across transformers, critical tasks increasingly challenged by data scarcity, rising demand volatility, and the integration of distributed energy resources[1]. Transformer overloads and phase imbalances remain persistent issues, leading to excessive energy losses, accelerated equipment degradation, and heightened risk of system instability[2]. These problems are particularly acute in looped or closed-loop distribution topologies, where chaotic load connections and incomplete metering data impede accurate load profiling and proactive asset management[3]. In such contexts, improper phase allocation can trigger recurrent fuse failures, frequent outages, and premature transformer failures, with replacement costs exceeding 10-20 million CFA francs per unit and most units rendered irreparable post-failure[4]. Yet, when operated within nominal limits, transformers can reliably serve for over 30 years[5], underscoring the economic and operational value of precision load optimization.

To mitigate these challenges, utilities and researchers have explored a range of strategies, from passive design techniques like star-connected secondary windings and neutral conductor sizing[6] to active management via load spreading and dynamic reconfiguration[7]. Advanced computational methods have also been deployed, including probabilistic frameworks such as Monte Carlo simulations, fuzzy logic, and risk-based transformer loading models that account for ambient temperature and load variability[8]. Optimization-based approaches for transformer siting, sizing, and load-center alignment have further demonstrated cost and efficiency gains in rural and radial networks[9]. Meanwhile, real-time monitoring innovations, such as online error detection in Capacitor Voltage Transformers (CVTs) have enhanced measurement fidelity and fault diagnostics[10].

Despite these advances, a critical gap persists: the simultaneous optimization of transformer loading and three-phase balancing under conditions of incomplete or uncertain load data, especially in looped networks where phase assignment is non-trivial[11]. Many existing methods either assume full observability or focus on isolated aspects, such as sizing without phase correction or harmonic mitigation without load redistribution[12]. Metaheuristic algorithms, including genetic algorithms and particle swarm optimization, have shown promise in distribution system

optimization[13], yet they often lack convergence guarantees or fine-grained local refinement under noisy or sparse inputs.

To bridge this gap, we propose a hybrid biogeography-gradient framework for load and phase optimization in power grids, integrating the global exploratory strength of Biogeography-Based Optimization (BBO)[14,15] with the local precision of gradient descent[16,17]. BBO excels in navigating complex, multimodal search spaces with minimal prior knowledge, ideal for data-limited scenarios, while gradient descent ensures rapid convergence to high-quality local optima once promising regions are identified. This synergy yields a robust, data-efficient optimizer capable of balancing phase loads and redistributing transformer assignments even with incomplete daily profiles.

Simulation results demonstrate transformative performance: a 49.99% reduction in phase imbalance, 28.71% fewer overloaded transformers (from a 68% baseline), and 10.86% fewer underloaded units (from 18%). Beyond technical gains, the framework supports scalable deployment through intuitive visualization tools and fault-monitoring modules, enabling operators to extend asset lifespans, reduce maintenance costs, and enhance service quality. By unifying metaheuristic adaptability with analytical rigor, this work establishes a foundation for intelligent, self-healing distribution systems, paving the way for real-time, AI-driven grid resilience in the face of growing uncertainty and complexity.

METHODOLOGY

The process begins with data collection, where the nominal power of transformers, actual power measured on each transformer, and actual load measured by phases are gathered. Next, the collected data undergoes load conditions evaluation, which includes verifying overloads, underloads, and phase imbalances. This evaluation helps identify any inefficiencies or issues in the transformer's operation. Based on the evaluation, optimization is performed to address these issues. The optimization focuses on load optimization and phase balancing to improve efficiency. The final goal is to ensure the transformers operate within optimal conditions, preventing overloads and imbalances.

Load Conditions Evaluation

In May 2022, a measurement campaign was conducted across 28 highly-loaded substations in the study area, a period known for peak network saturation. The results were alarming. Assessments of the looped network (Table 1) revealed that 68% (19 units) were overloaded, while a significant 85.71% (23 units) suffered from phase unbalance, with most operating beyond their nominal capacity. This irregular loading has severe consequences. Oversizing leads to financial waste and unnecessary losses, while undersizing forces constant overloading. This results in excessive winding heat, triggering protective shutdowns, and the accelerated deterioration of insulation. Ultimately, this leads to a permanent loss of lifespan and risks dielectric failure. These critical issues drive the urgent need, as noted by researchers[18–20], to optimize transformer power to ensure network reliability and longevity.

TABLE 1. Measurements taken on the looped distribution network.

Transformer N°	P_{nom} (KVA)	Measured load currents			P_{meas} (KVA)	Average load rate (%)
		I_a (A)	I_b (A)	I_c (A)		
N46	400	660.00	570.00	670.00	495.00	123.75
T75	630	664.00	641.00	68.00	530.27	84.17
T48	400	666.00	573.00	669.00	465.36	116.34
T03	630	36.43	520.00	328.80	335.03	53.00
T05	400	806.50	620.30	590.50	582.50	145.50
T07	1000	638.70	815.60	610.20	684.66	68.46
T10	1000	537.00	531.30	440.70	640.80	64.08
T17	400	623.10	477.60	668.90	463.40	115.90
T18	500	359.00	594.40	443.90	420.04	84.00
T20	200	324.80	317.30	315.10	236.00	118.13
T24	400	137.95	156.74	149.84	177.19	44.29
T25a	630	926.03	1 078.10	1 004.00	773.07	122.70
T28	1000	926.90	775.60	892.40	1 047.84	105.00
T31	400	601.70	626.80	714.00	541.71	135.42
T33	100	90.50	228.50	182.50	158.30	158.00

T35	400	434.10	615.30	407.70	421.00	105.30
T80	630	750.40	697.30	691.90	491.29	77.90
T83b	250	335.90	377.40	385.15	312.23	124.89
T99	400	669.00	578.00	679.00	465.36	116.34
T87	250	344.80	317.80	325.10	295.18	118.07
T71	250	364.50	337.60	375.80	312.27	124.91
N49	400	237.95	256.74	249.84	335.03	83.76
N52	400	808.50	618.90	598.70	584.66	146.16
N55	400	603.20	636.30	712.90	540.80	135.20
N47	160	75.47	97.35	91.95	115.97	72.48
N48	400	659.00	576.00	673.00	473.07	118.27
TX	400	658.00	568.00	667.00	491.29	122.82
H61	160	90.50	218.50	192.50	198.79	124.24

Phase Imbalance and Load Optimization Methodology

Optimally distributing transformer loads is vital for efficient, reliable electrical systems. By integrating real-world data with intelligent learning models, this approach significantly enhances load management, ensuring adequate service and improving network performance[21–23]. Phase imbalance (Δphase) is a critical parameter in electrical systems, defined as the maximum absolute difference between phase currents (Equation 1). Real-time monitoring relies on this metric, while standards like IEC 61000-4-30 use symmetrical components for formal assessment. To ensure safety, the total phase current (I_{total}) must not exceed the predefined capacity (I_{max}), as per IEC 60364-8-1 and NEC Article 220 (Equation 2). The apparent power (P_{total}) is calculated using optimized currents and nominal voltage (Equation 3), following IEC 60076-1 and IEEE 1459. Additionally, a temperature correction factor (K_T) adjusts transformer capacity based on ambient conditions (Equation 4), aligning with IEC 60076-7 and IEEE C57.91. This framework ensures efficient and reliable transformer operation under varying load and environmental conditions.

Standard methods such as IEC 61000-4-30, employ symmetrical components for formal unbalance assessment[11]. Phase imbalance ($\boldsymbol{\Delta_{phase}}$) can be expressed as Equation (1):

$$\Delta_{phase} = \varepsilon_{ch} = \max\left(|I_a - I_b|, |I_b - I_c|, |I_c - I_a|\right) \quad (1)$$

Where: I_a, I_b, I_c are the load current of the three phases.

The total phase current (I_{total}) sum ($I_a + I_b + I_c$) must not go over the predefined current capacity (I_{max}) of the equipment, as specified in IEC 60364-8-1[24,25] and NEC Article 220 for load safety[26]. Maximum load constraint (I_{ma}) is given as Equation (2):

$$I_{total} = I_a + I_b + I_c \leq I_{max} \quad (2)$$

Where: I_{max} is the current capacity based on the nominal power.

The power (in kVA) can be calculated for each transformer and each phase from the optimized currents, assuming a nominal voltage $\mathbf{V_{nom}}$, where the voltage is expressed in volts and the currents in amperes.

The total apparent power of the three-phase system was determined using P_{total}, consistent with IEC 60076-1 and IEEE 1459 definitions for three-phase power[27]. Transformer loading was verified using the apparent power $\mathbf{P_{total}}$, as recommended in ABB's Transformer Handbook[28] written as Equation (3) :

$$P_{total} = \frac{\sqrt{3} \times V_{nom} \times I_{opt}}{1000} \quad (3)$$

Where: $\mathbf{V_{nom}}$ is expressed in volts while $\mathbf{I_{opt}}$ is in amperes.

The integration of a correction coefficient $\mathbf{K_T}$ allows the adjustment of the transformer's maximum capacity based on the ambient temperature at the study location. The temperature correction factor $\mathbf{K_T}$, consistent with derating principles in IEC 60076-7 and IEEE C57.91[2930,31] is given in the Equation (4):

$$K_T = 1 - 0{,}005 \times (T_{avg} - 25) \quad (4)$$

A Hybrid Metaheuristic-Gradient Framework for Complex Optimization

Constrained nonlinear optimization problems, common in engineering, are notoriously difficult due to multiple local optima and complex constraints. Traditional solvers often yield suboptimal results. To overcome this, we propose a hybrid framework that synergistically combines the global exploration power of the BBO metaheuristic[14,15,32,33] with the local precision of MATLAB's F_{mincon} solver[34,35]. BBO first navigates the search space broadly to identify promising regions, effectively escaping local traps. F_{mincon} then refines these solutions, leveraging its strength in handling intricate constraints with high accuracy. This global-to-local strategy ensures robust convergence and superior solution quality for the most challenging problems, achieving what either method could not accomplish alone.

Biogeography-Based Optimization Algorithm

BBO algorithm[36] is a powerful population-based metaheuristic inspired by the science of species distribution across ecosystems[37]. In BBO, each candidate solution is conceptualized as a "habitat" whose quality is measured by a Habitat Suitability Index (HSI), analogous to a fitness function. The algorithm's core mechanism is a probabilistic migration process, where high-HSI habitats (superior solutions) emigrate their good traits, while low-HSI habitats are more likely to immigrate and receive these beneficial characteristics. This dynamic exchange, mimicking natural biogeography, effectively drives the population toward global optima. A mutation operator is also incorporated to preserve population diversity and prevent premature convergence. BBO's unique migration model provides a distinct and effective balance between exploring new regions and exploiting known good solutions, making it particularly adept at navigating complex, high-dimensional problems. Its competitive performance and practical robustness have been validated in real-world engineering applications, such as aircraft engine health monitoring[14,15,32].

Nonlinear Optimization of Phase Load Balance

The optimization employs The **F_{mincon}**, a gradient-based solver for nonlinear constrained problems[34,35], to minimize an objective function subject to variable bounds, linear constraints ($A \times x \leq b \; and \; A_{eq} \times x = b_{eq}$), and nonlinear constraints ($c(x) \leq 0$ and $c_{eq}(x) = 0$). The objective function combines current tracking accuracy with phase imbalance minimization using calibrated weighting factors (α,β)[30,31]:

$$f(x) = \alpha . \sum_{i=1}^{N} \sum_{j \in (a,b,c)} (I_{ij}^{opt} - I_{ij}^{meas})^2 + \beta . \sum_{i=1}^{N} std(I_{ia}, I_{ib}, I_{ic}) \quad (5)$$

Where:

N = number of transformers in the distribution network;
x = vector of optimized phase loads (84 variables: 3 phases x 28 transformers)
I_{ij}^{opt} = optimized load currents for transformer *i* on phase *j*
I_{ij}^{meas} = measured current for transformer *i* on phase *j*
$std(I_{ia}, I_{ib}, I_{ic})$ = standard deviation of phase currents (quantifying imbalance)
(α, β) = weighting coefficients balancing tracking accuracy and symmetry

Operational constraints ensure compliance with transformer ratings per IEC 60076-1, where phase currents satisfy [38 39]:

$$I_{min} \leq I_{ij}^{opt} \leq I_{max} \quad (6)$$

Where

$I_{max} = \frac{P_{nom}}{\sqrt{3}.V.cos\varphi}$: derived from the fundamental relationship between rated power, voltage, and current in three-phase systems
I_{min} = 0: assumes no reverse power flow or minimum load constraints. If bidirectional power flow is allowed (e.g., in distributed generation), I_{min} may be negative
V = Line Voltage
$cos\varphi$ = cosϕ = power factor (unity minimizes Imax).

This formulation balances measurement fidelity against phase symmetry requirements while maintaining thermal and operational compliance across the distribution network.

Workflow of Transformer Load Optimization

The workflow begins with data-informed initialization, where diverse yet feasible phase-load vectors are generated using transformer ratings, voltage/current measurements, and load forecasts. This ensures broad exploration of the solution space. Next, dynamic overload/imbalance screening rapidly assesses system risk by fusing overload, imbalance, and forecast error metrics, adjusting search intensity and flagging constrained assets. A multi-objective function with adaptive weighting then guides optimization, balancing current-tracking fidelity, phase balance, losses, voltage deviation, and constraint adherence. Weights shift dynamically based on time-of-day, congestion, and reliability needs. The core search employs an enhanced BBO featuring adaptive migration rates, multi-swarm diversity, chaotic exploration, constraint-aware repair, and early stopping, yielding a diverse set of high-quality candidates approximating the Pareto front. From these, best-candidate selection identifies top compromises using Pareto-knee or fairness criteria, preserving a few robust options. Each undergoes local refinement via $\mathbf{F_{mincon}}$, a gradient-based optimizer that fine-tunes solutions under full physical constraints for precision and feasibility. Before finalizing, a robustness check stress-tests candidates against load variations, forecast errors, and noise. Unstable solutions trigger re-optimization with adjusted parameters. If validated, the algorithm proceeds to finalization, delivering optimized phase allocations, current estimates, loss/voltage profiles, and interpretable summaries for operators. Designed for real-time continuity, the workflow repeats cyclically, using prior results as seeds to adapt proactively to evolving grid conditions, ensuring sustained balance and resilience without reactive interventions. This integrated approach harmonizes global exploration, adaptive objectives, and local precision to manage transformer overloads and phase imbalances effectively under uncertainty. The optimization workflow of transformers' load.

Quantifying and Validating Phase Balance

In three-phase power systems, current imbalance threatens efficiency, equipment longevity, and stability, causing overheating, voltage distortion, and excess losses. To address this, the Current Unbalance Factor (CUF) serves as a standardized KPI, quantifying imbalance as the percentage deviation between max/min and average phase currents (per ANSI C84.1-1995)[40,41]:

$$\text{CUF}\ (\%) = \frac{\text{Max Phase Current} - \text{Min Phase Current}}{\text{Average Phase Current}} \times 100 \tag{7}$$

A CUF of 0% indicates perfect balance and higher values signal greater risk. However, diagnosis alone is insufficient. The Current Unbalance Factor Reduction (CUFR) measures the effectiveness of corrective actions, such as load redistribution or optimization algorithms, by comparing baseline and post-intervention CUF values:

$$\text{CUF}_{\text{Red}}\ (\%) = \frac{\text{Baseline CUF} - \text{Optimized CUF}}{\text{Baseline CUF}} \tag{8}$$

A positive CUFR confirms improvement while a negative value warns of worsening imbalance. Together, CUF and CUFR form a robust diagnostic and validation framework, enabling engineers to not only detect phase imbalance but also objectively assess mitigation strategies[42]. This dual-metric approach supports data-driven decisions, ensuring interventions enhance system performance, reliability, and operational safety while providing clear, quantifiable evidence of success[43].

RESULTS AND DISCUSSION

Transformer Load Optimization

Optimized Transformer Power within the Looped Network

The implemented methodology successfully optimized transformer power distribution within the looped network, yielding improved load profiles across all phases. Analysis of optimized versus nominal powers (Fig.1) reveals significant imbalances. Several transformers (T03, T07, T10, T24, T80) are substantially oversized, allowing for immediate capacity reduction or increased loading up to 90%. Conversely, transformers N52, N55, N48, and TX are overloaded and require replacement with higher-capacity units or permutation with the underloaded transformers. For the remaining units, load transfers to adjacent transformers should balance the network. Applying this systematic optimization across the entire network promises widespread efficiency gains, showcasing the technique's universal applicability to electrical distribution systems.

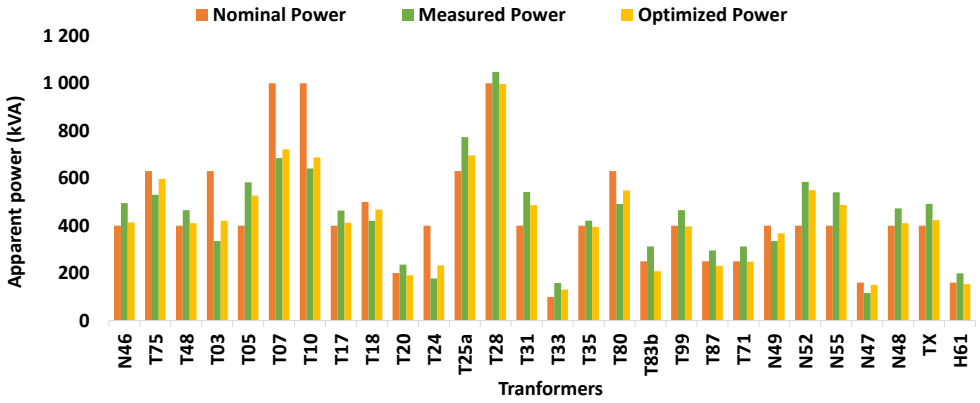

FIGURE 1. Optimized transformer power distribution within the looped network.

Optimized Transformer Load Current within the Looped Network

Optimization results, as illustrated by Fig. 2, reveal markedly improved load current profiles per transformer phase, achieved by swapping and adjusting loads. This enhances phase balancing, ensuring normal transformer operation in looped networks. For efficient management, install a monitoring system with appropriate measurement equipment and analytical tools to detect anomalies in real-time, enabling proactive maintenance and reliable performance.

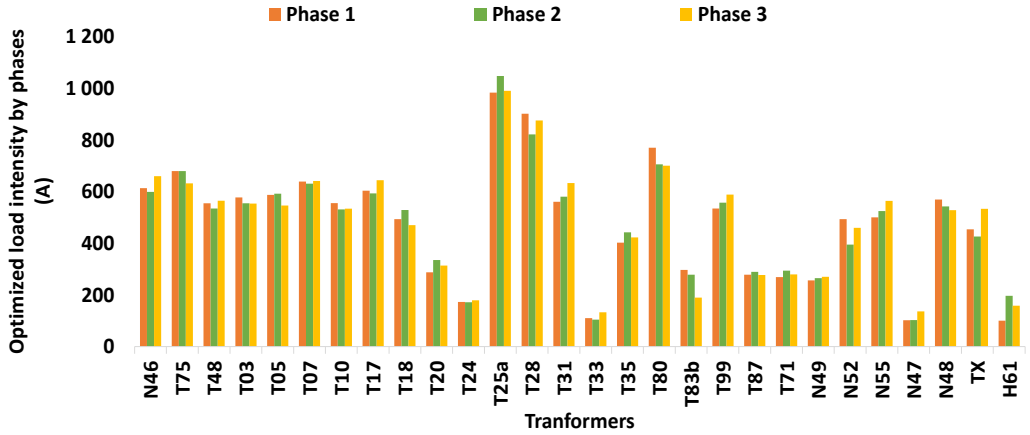

FIGURE 2. Optimized Transformer load current within the looped network.

Intelligent Transformer Load Monitoring with Real-Time Anomaly Detection via BBO+F_{mincon} Algorithms

Transformer load monitoring employs three current transformers per phase and a three-phase power meter, with data analyzed via BBO + F_{mincon} algorithms for anomaly detection. The process starts by defining objectives to select and install suitable equipment, enabling continuous data recording. Key indicators include measured power (P_{meas}) versus nominal power (P_{nom}), and current imbalance ($\varepsilon_{ch} > 0.1$, derived from phase currents I_a, I_b, I_c). Alerts trigger if $P_{meas} > 0.9P_{nom}$ and $\varepsilon ch > 0.1$; otherwise, analysis loops. Post-alert, comprehensive result analysis allows objective refinement, fostering continuous improvement in electrical system monitoring and management.

Reduction in Current Unbalance across Transformer Fleet

Across the transformer fleet, the optimization campaign achieved a striking 55.3 % average drop in Current Unbalance Factor (CUF), falling from 45.1 % in the baseline to 32.5 %. Baseline CUFs spanned 7.6 % to 82.6 %,

revealing a mix of well-balanced units and highly unbalanced ones. Post-optimization, the range tightened to 1.7 %–63.3 %, with the most dramatic improvement of 94 % on the worst-case transformer and a modest 16 % gain on the least-affected unit. The greatest benefits surfaced for transformers that were severely unbalanced at start (CUF ≥ 74 %), the top seven, T07, T03, T35, T18, T10, T05, and T17, each saw reductions between 74 % and 94 % as outlined by Table 2. Five transformers (T20, T80, T83b, N47, TX) were omitted from the final tally because their post-optimization CUFs behaved atypically. N47 and T80 exhibited minimal change (≤ 5 pp), while T20, T83b, and TX were deliberately allowed to worsen (≥ 10 pp) to achieve substantial RI² loss reductions (51 % for T83b and TX). This trade-off is justified by the larger cost savings and remains within safe operating limits. The algorithm's focus on total cost savings, rather than perfect balance, mirrors real-world operational priorities. These results demonstrate that targeted phase-balancing, even when coupled with strategic load reductions, can deliver significant reliability improvements while preserving economic efficiency across a diverse transformer portfolio.

TABLE 2. Top 7 performers achieved reductions of 74–94%.

Transformer	Baseline CUF (%)	Optimized CUF (%)	CUF Reduction (%)
T07	29.8%	1.7%	94%
T03	48.4%	4.2%	91%
T35	42.7%	9.5%	78%
T18	50.5%	11.,8%	77%
T10	19.1%	4.5%	76%
T05	32.1%	8.0%	75%
T17	32.4%	8.3%	74%

Optimization of Current Load and Phase Unbalance across all Transformers

The optimization process successfully reduced both current load and phase unbalance across all transformers, enhancing system efficiency and minimizing losses. Current load reductions varied among units, with some experiencing substantial decreases while others showed moderate improvements. The Current Unbalance Factor (CUF) reduction was most dramatic for transformers with high initial imbalance, reaching 94% for T07, while transformers with lower baseline unbalance achieved smaller but still meaningful improvements, with T71 showing 16% reduction.

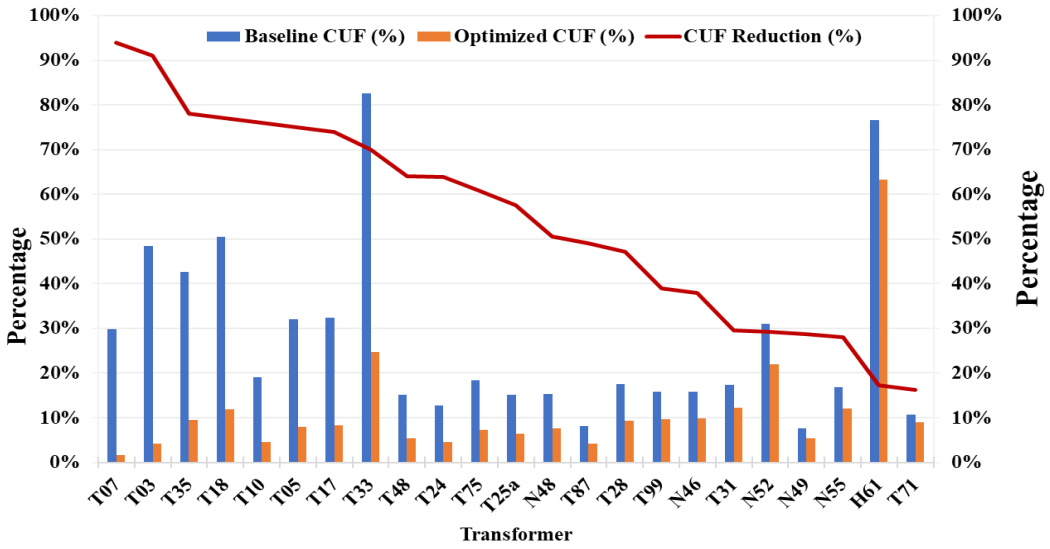

FIGURE 3. Baseline CUF, optimized CUF, and reduction percentages for each transformer.

Figure 3 illustrates the baseline CUF, optimized CUF, and reduction percentages for each transformer, revealing consistent improvements across the entire fleet. Transformers with the highest initial CUF values, indicating severe phase imbalance, achieved reductions often exceeding 70-90%. This pattern demonstrates that the optimization algorithm was particularly effective at addressing the most problematic units while still providing benefits to all

transformers. The strong correlation between current load reduction and CUF improvement confirms that the phase balancing intervention successfully achieved its dual objectives of load balancing and loss minimization throughout the transformer network.

CONCLUSION

This work presents a hybrid optimization framework that synergizes Biogeography-Based Optimization with gradient descent to address phase imbalances and transformer over/underloading in distribution networks, critical challenges intensified by incomplete load data. Simulation results demonstrate transformative improvements: a 49.99% reduction in phase imbalance, 28.71% fewer overloaded transformers (from 68% baseline), and 10.86% fewer underloaded units (from 18% baseline). By combining global search robustness with local precision, the framework enhances grid reliability, reduces energy losses, and extends infrastructure lifespan, yielding tangible operational and economic benefits. Integrated visualization tools further empower operators with actionable insights for proactive management. The methodology offers a scalable, data-resilient solution for modern grids facing rising complexity from distributed generation and variable demand. Future work will explore quantum-inspired or ensemble metaheuristics coupled with deep reinforcement learning to enable real-time, adaptive load rebalancing. Ultimately, this research advances hybrid AI as a cornerstone for self-healing, intelligent distribution systems bridging simulation-driven innovation to field-deployable resilience and accelerating the transition toward sustainable, consumer-centric smart grids.

REFERENCES

1. J. Gallegos, P. Arévalo, C. Montaleza, and F. Jurado, Sustain. 16, (2024).
2. T. Bharath Kumar and M. Ramamoorty, in Lect. Notes Electr. Eng. (2021).
3. C. Yang, Y. Sun, Y. Zou, F. Zheng, S. Liu, B. Zhao, M. Wu, and H. Cui, Energies 16, 1 (2023).
4. A.M. Agwa and A.A. El-Fergany, Sustain. 15, (2023).
5. Z. Janic, N. Gavrilov, and I. Roketinec, Energies 16, (2023).
6. E.P. López, A.L. Vinet, V.L. Martínez, J.M. Romeu, and I.V. Salazar, Electr. Power Syst. Res. 215, (2023).
7. Y. Zerguit, Y. Hammoudi, I. Idrissi, and M. Derrhi, J. Theor. Appl. Inf. Technol. 101, (2023).
8. P. Dupis, R. Gianto, and J. Junaidi, Telecommun. Comput. Electr. Eng. J. 1, (2024).
9. L.M. Adesina, A. Abdulkareem, O. Ogunbiyi, and O. Ibrahim, MethodsX 7, (2020).
10. Z. Zhu, L. Heng, and L. Binbin, Rev. Sci. Instrum. 95, (2024).
11. V.A. Jimenez, A.L.E. Will, and D.F. Lizondo, Int. J. Electr. Power Energy Syst. 137, 107691 (2022).
12. H. Rezk, A.G. Olabi, E.T. Sayed, and T. Wilberforce, Sustain. 15, (2023).
13. A.M. Nassef, M.A. Abdelkareem, H.M. Maghrabie, and A. Baroutaji, Sustain. 15, (2023).
14. R. Vargas, L.H. MacEdo, J.M. Home-Ortiz, J.R.S. Mantovani, and R. Romero, IEEE Trans. Smart Grid 12, (2021).
15. J. Li, X. Wang, C. Xie, J. Han, C. Mao, X. Liu, D. Wang, Y. Zhang, Z. Guan, and X. Zhang, in Proc. 2021 IEEE 4th Int. Electr. Energy Conf. CIEEC 2021 (2021).
16. C. Bai, Q. Li, W. Zhou, B. Li, and L. Zhang, Energy Reports 8, (2022).
17. L. Fu and D.D. Ge, J. Oper. Res. Soc. China 11, (2023).
18. S.K. Chowdhury, H. Kobayashi, and K. Kondo, IEEJ J. Ind. Appl. 9, (2020).
19. J.Z. Balanta, S. Rivera, A.A. Romero, and G. Coria, Energies 16, (2023).
20. M.I. Hassan, N. Keshmiri, A.D. Callegaro, M.F. Cruz, M. Narimani, and A. Emadi, IEEE Open J. Ind. Electron. Soc. 2, (2021).
21. S. Akhtar, M. Adeel, M. Iqbal, A. Namoun, A. Tufail, and K.H. Kim, Energy Reports 10, (2023).
22. M. Bjelić, B. Brković, M. Žarković, and T. Miljković, Int. J. Electr. Power Energy Syst. 156, (2024).
23. S. Barja-Martinez, M. Aragüés-Peñalba, Í. Munné-Collado, P. Lloret-Gallego, E. Bullich-Massagué, and R. Villafafila-Robles, Renew. Sustain. Energy Rev. 150, (2021).
24. L. Martirano, A. Ruvio, M. Manganelli, F. Lettina, A. Venditti, and G. Zori, IEEE Trans. Ind. Appl. 57, (2021).
25. L. Martirano, A. Ruvio, M. Manganelli, F. Lettina, A. Venditti, and G. Zori, in 2020 IEEE Ind. Appl. Soc. Annu. Meet. IAS 2020 (2020).
26. S. Bogarra, J. Saura, and A. Rolán, Sensors 22, (2022).

27. G. Artale, G. Caravello, A. Cataliotti, V. Cosentino, D. Di Cara, S. Guaiana, N. Panzavecchia, and G. Tine, IEEE Trans. Instrum. Meas. 70, (2021).
28. M. V. Czernorucki, M.B.C. Salles, E.C.M. Costa, A.S. Melo, and L. Piegari, IEEE Access 10, (2022).
29. S. Hu, R. Zhu, G. Li, L. Song, J.C. Solano, T. Montaño, J. Maldonado-Correa, A. Ordóñez, M. Pesantez, G. Stavarache, S. Ciortan, E. Rusu, A. Diaconita, G. Andrei, L. Rusu, J. Zhang, J. Lu, J. Pan, Y. Tan, X. Cheng, Y. Li, F. Attig-Bahar, U. Ritschel, P. Akari, I. Abdeljelil, M. Amairi, X. Wei, Y. Xiang, J. Li, J. Liu, H. Chen, Y. Birkelund, F. Yuan, A. Hutchinson, D.T. Gladwin, Z. Abada, M. Bouharkat, D. Lyners, H. Vermeulen, M. Groch, M. Pellegrini, A. Guzzini, C. Saccani, Q. Yu, Y. Liu, Z. Jiang, L. Li, Y. Zhang, M. Guo, N. Gylling, A. Serban, L.S. Paraschiv, S. Paraschiv, M. Sumair, T. Aized, S.A.R. Gardezi, S.U. ur M.S. Rehman, S.U. ur M.S. Rehman, M. Adnan, J. Ahmad, S.F. Ali, M. Imran, T. Khan, J. Taweekun, T. Theppaya, A. De Meij, J.F. Vinuesa, V. Maupas, J. Waddle, I. Price, B. Yaseen, A. Ismail, S.A. Mathew, V.E.N. Mariappan, S. Paraschiv, L.S. Paraschiv, A. Serban, A.G. Cristea, K. Zhang, X. Yu, S. Liu, X. Dong, D. Li, H. Zang, R. Xu, X. Yu, S. Liu, X. Dong, H. Zang, R. Xu, J. Taghinezhad, S. Sheidaei, Z.H. Hulio, F. Topaloğlu, H. Pehlivan, P. Enevoldsen, and F.-H. Permien, Energy Reports 7, 1 (2021).
30. L. Wang, X. Zhang, R. Villarroel, Q. Liu, Z. Wang, and L. Zhou, IET Gener. Transm. Distrib. 14, (2020).
31. G. Gmati, U.M. Rao, I. Fofana, P. Picher, O. Arroyo-Fernàndez, and D. Rebaine, Energies 16, (2023).
32. Z. Guan, P. Tang, C. Mao, D. Wang, L. Wang, W. Liu, M. Du, J. Li, and X. Wang, IEEE Access 12, (2024).
33. O. Bamisile, C. Dongsheng, J. Li, H. Adun, R. Olukoya, O. Bamisile, and Q. Huang, Energy Reports 9, (2023).
34. M. Vadood and A. Haji, Coatings 12, (2022).
35. B. Karthick, J. Manag. Anal. 10, (2023).
36. Z. Zhang, Y. Gao, and W. Zuo, IEEE Access 10, (2022).
37. G. Gizachew, ASEAN J. Sci. Eng. 2, (2022).
38. M. Tabrez, P.K. Sadhu, M.S.H. Lipu, A. Iqbal, M.A. Husain, and S. Ansari, Machines 10, (2022).
39. T. Hidayat, B.W. Dionova, S. Wilyanti, and M.N. Mohammed, Eksergi 18, (2022).
40. S. Singh, Int. J. Res. Appl. Sci. Eng. Technol. 7, (2019).
41. Denis, E.W. Sinuraya, M. Soemantri, and I.R. Rafif, in J. Phys. Conf. Ser. (2022).
42. M. Abubakar, H. Renner, and R. Schürhuber, Energies 16, (2023).
43. R. Benato, G. Gardan, and L. Rusalen, IEEE Access 9, (2021).